Monthly Notices
of the
ROYAL ASTRONOMICAL SOCIETY

MNRAS **464,** 3060–3070 (2017)
Advance Access publication 2016 September 30

doi:10.1093/mnras/stw2483

Lack of nuclear clusters in dwarf spheroidal galaxies: implications for massive black holes formation and the cusp/core problem

Manuel Arca-Sedda★ and Roberto Capuzzo-Dolcetta

Department of Physics, Sapienza University of Rome, Piazzale Aldo Moro 5, I-00185 Rome, Italy

Accepted 2016 September 28. Received 2016 September 27; in original form 2016 July 2

ABSTRACT

One of the leading scenarios for the formation of nuclear star clusters in galaxies is related to the orbital decay of globular clusters (GCs) and their subsequent merging, though alternative theories are currently debated. The availability of high-quality data for structural and orbital parameters of GCs allows us to test different nuclear star cluster formation scenarios. The Fornax dwarf spheroidal (dSph) galaxy is the heaviest satellite of the Milky Way and it is the only known dSph hosting five GCs, whereas there are no clear signatures for the presence of a central massive black hole. For this reason, it represents a suited place to study the orbital decay process in dwarf galaxies. In this paper, we model the future evolution of the Fornax GCs simulating them and the host galaxy by means of direct *N*-body simulations. Our simulations also take into account the gravitational field generated by the Milky Way. We found that if the Fornax galaxy is embedded in a standard cold dark matter halo, the nuclear cluster formation would be significantly hampered by the high central galactic mass density. In this context, we discuss the possibility that infalling GCs drive the flattening of the galactic density profile, giving a possible alternative explanation to the so-called cusp/core problem. Moreover, we briefly discuss the link between GC infall process and the absence of massive black holes in the centre of dSphs.

Key words: galaxies: dwarf – galaxies: evolution – galaxies: kinematics and dynamics – galaxies: nuclei – galaxies: star clusters.

1 INTRODUCTION

Among all the dwarf spheroidal (dSph) satellite galaxies of the Milky Way (MW), Fornax is the only one hosting five globular clusters (GCs), at projected distances from its centre smaller than 1 kpc. On the other hand, this galaxy does not exhibit any evidence of a clear central overdensity or the presence of a massive black hole (MBH). Several works have pointed out that the Fornax dSph lies inside a huge dark matter halo (DMH) (Mateo 1998). The presence of GCs, namely Fornax 1, 2, 3, 4 and 5, represents an open puzzle since the action of dynamical friction (df) should have dragged them into the galactic centre a few Gyr ago. Indeed, these old, metal-poor GCs have ages exceeding 10 Gyr (Buonanno et al. 1998, 1999; Larsen, Strader & Brodie 2012), a value significantly larger than their df decay time (Tremaine 1976; Oh, Lin & Richer 2000). However, it has been widely demonstrated that the standard approach for studying the df process, developed so far by Chandrasekhar (1943), poorly describes the motion in axisymmetric and triaxial (Ostriker, Binney & Saha 1989; Pesce, Capuzzo-Dolcetta & Vietri 1992) or spherical and cuspy galaxies (Antonini & Merritt 2012; Arca-Sedda & Capuzzo-Dolcetta 2014b; Petts, Gualandris & Read 2015; Petts, Read & Gualandris 2016). Moreover, since the orbital energy loss primarily depends on the host galaxy structure, a reliable description of the GC motion requires a detailed knowledge of the Fornax mass distribution. Though the Fornax dSph is believed, like all the dSphs, to be enclosed within a DMH, its density profile seems to differ significantly from the standard prediction of the Λ cold dark matter (ΛCDM) paradigm, $\rho(r) \propto r^{-1}$ (Navarro, Frenk & White 1996; Walker et al. 2009). Indeed, observational constraints suggest a flatter density profile (Flores & Primack 1994; Moore 1994; Gilmore et al. 2007; Cowsik et al. 2009; Jardel & Gebhardt 2012). Hence, the study of the dynamical evolution of Fornax GCs can shed light on the structure of dSph galaxies, and, in particular, on their DM content.

Currently, several scenarios have been proposed and debated to explain the dynamical evolution of the Fornax and its GCs.

For instance, some authors proposed that this galaxy is characterized by a flat density profile, with a core extending up to 300 pc (Strigari et al. 2006), while others argued that it is the product of a merger event (Coleman et al. 2004; Olszewski et al. 2006; Yozin & Bekki 2012). Angus & Diaferio (2009) proposed, instead, that the assumption of modified Newtonian dynamics (Milgrom 1983) leads to a direct interpretation of the observed dynamical status of

★ E-mail: m.arcasedda@gmail.com

the Fornax GCs. Another possibility relies upon that df halts its role within the region where the density profile flattens (Goerdt et al. 2006; Read et al. 2006b; Gualandris & Merritt 2008; Arca-Sedda & Capuzzo-Dolcetta 2014b).

Using recent observational data, in a companion paper we revisited the so-called 'timing' problem, showing that all the GCs have been formed within the Fornax tidal radius, even in the case of a standard CDM density profile for the Fornax halo (Arca-Sedda & Capuzzo-Dolcetta 2016).

Intriguingly, the presence of five GCs moving in the inner region of the galaxy coincides with the absence of a bright nucleus. Bright nuclei, often referred to as nuclear clusters (NCs), are very dense stellar systems with masses in the range 10^8–10^{11} $M_\odot$ observed in galaxies of all the Hubble types (van den Bergh 1986; Côté et al. 2004, 2006; Turner et al. 2012). Some authors proposed an '*in situ*' origin for NCs (McLaughlin, King & Nayakshin 2006; Nayakshin, Wilkinson & King 2009; Aharon & Perets 2015); another possibility is that GCs decay towards the centre of their host galaxy, where they collide and merge, driving the formation of an NC and, even, the accretion of a black hole seed therein (Tremaine, Ostriker & Spitzer 1975; Capuzzo-Dolcetta 1993). This channel of formation, named 'dry-merger' scenario, has been successfully investigated both on a theoretical and a numerical side (Capuzzo-Dolcetta & Miocchi 2008; Antonini et al. 2012; Antonini 2013; Arca-Sedda & Capuzzo-Dolcetta 2014a), and satisfactorily explains the observed correlations among NC properties and those of their host galaxies (Arca-Sedda & Capuzzo-Dolcetta 2014b; Leigh, Böker & Knigge 2012; Scott & Graham 2013). Recently, some authors have shown that the tidal forces induced by a very massive BH can tidally disrupt the infalling GCs, thus suppressing the formation of an NC (Bekki & Graham 2010; Antonini 2013; Arca-Sedda & Capuzzo-Dolcetta 2014a; Arca-Sedda et al. 2015; Arca-Sedda, Capuzzo-Dolcetta & Spera 2016).

In a recent paper, Arca-Sedda et al. (2015) investigated the future evolution of the 11 young massive clusters located in the dwarf starburst galaxy Henize 2-10. This work is the first showing that the formation of an NC is a process that can occur in a galaxy containing a pre-existing MBH, even if the tidal field induced by the massive BH and by the background stars can significantly alter the NC formation process. In the same framework, in this paper we simulate the future evolution of the Fornax globular cluster system (GCS) making use of direct *N*-body modelling. The availability of high-quality data on the structural and orbital parameters of GCs and on the host galaxy would allow us to investigate whether their future evolution may lead to the formation of a nucleated region. This has a double aim: (i) study the ongoing orbital decay process and put constraints on the possible formation of NCs in dSph galaxies and (ii) extrapolate our results backward in time in order to obtain hints about the origin of GCs and past evolution.

The paper is organized as follows: in Section 2, we describe the matter distribution adopted to model the galaxy and the GCs, and the numerical method used; in Section 3, we present the results of the *N*-body simulations and discuss them in Section 5; finally, in Section 6, we draw the conclusions of this work.

2 MODELLING THE MILKY WAY, THE FORNAX dSph AND THEIR GLOBULAR CLUSTERS

In this work, we present results from a series of direct *N*-body simulations in which we modelled the orbital decay of the five GCs orbiting in the Fornax dSph galaxy. To carry out the simulations, we used the direct *N*-body code HIGPUS (Capuzzo-Dolcetta, Spera & Punzo 2013), a sixth-order Hermite integrator with block time-step, which runs on graphic processing units, fully exploiting the advantages of parallel machines.

Table 1. Main parameters of the MW profile. Column 1: component of the MW. Column 2: mass scale of the component. Columns 3–4: length-scales of the component.

	M (10^{10} $M_\odot$)	a (kpc)	b (kpc)
Bulge	1.4	0.39	–
Disc	8.6	5.32	0.25
Halo	11	12	100

In all the simulations performed, the MW is modelled as an external, analytical, field, whereas the Fornax dSph and all the GCs have been represented self-consistently as N 'particles'. The number of particles that should be used for modelling the whole dSph exceeds 10^8, which is too much to allow a reasonable computational time. To overcome this problem, we (i) limited the representation of the galaxy to an inner region of ∼2 kpc, as explained more in detail below, and (ii) we allowed a difference between the individual mass of the particles in the dSph, m_F, and in the GCs, m_{GC}, such that $m_F/m_{GC} = 10$.

This implies a number of particles which is, in the smallest cluster, greater than 3×10^3. The evaporation time, which is the time-scale over which two-body relaxation is at all important, is ∼2 Gyr for the smallest cluster. Consequently, the evaporation time for all the clusters is significantly larger than the time over which they reach the Fornax centre, thus avoiding possible spurious effects of relaxation due to an exceedingly small number of particles.

2.1 The Milky Way model

The MW tidal field was modelled using the Allen & Santillan (1991) density profile, given by the sum of three different components, bulge, disc and halo. The galactic bulge is represented as a Plummer sphere (Plummer 1911):

$$\Phi_b(r) = -\frac{M_b}{\sqrt{r^2 + a_b^2}}, \tag{1}$$

the galactic disc is represented by a Miyamoto & Nagai (1975) law:

$$\Phi_d(x, y, z) = -\frac{M_d}{\sqrt{x^2 + y^2 + \left(a_d^2 + \sqrt{z^2 + b_d^2}\right)^2}}, \tag{2}$$

and the halo is described by a Navarro et al. (1996) profile:

$$\Phi_h(r) = -\frac{M_h (r/a_h)^{2.02}}{r(1 + (r/a_h)^{1.02})} - \frac{M_h}{1.02 a_h}\left[F(r) - F(b_h))\right], \tag{3}$$

where $F(r)$ is defined as

$$F(r) = -\frac{1.02}{1 + (r/a_h)^{1.02}} + \ln\left[1 + (r/a_h)^{1.02}\right]. \tag{4}$$

In equations (1) – (4), a_b, a_d, b_d, a_h are scalelengths, while M_b, M_d and M_h are masses, all listed in Table 1. We notice here that we used the same parameters as adopted in Arca-Sedda & Capuzzo-Dolcetta (2016).

In order to properly describe the motion of Fornax around the MW, we selected the following initial conditions (ICs) in the MW reference frame:

$$\boldsymbol{R}_{F0}(\mathrm{kpc}) = (0, 66, 220), \tag{5}$$

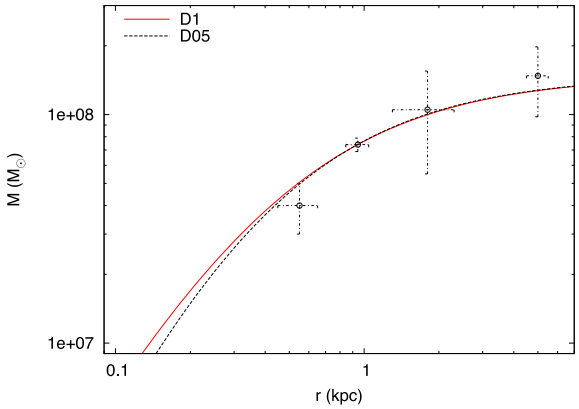

Figure 1. Cumulative mass profile for model D05 (straight red line) and model D1 (dotted black line) compared with observational data provided by Walker et al. (2009), Wolf et al. (2010), Walker & Peñarrubia (2011) and Cole et al. (2012).

$$\boldsymbol{V}_{\rm F0}(\rm km\,s^{-1}) = (-206, 0, 193). \tag{6}$$

This choice implies a pericentre and velocity in agreement with observational estimates (Buonanno et al. 1999; Dinescu et al. 2004).

Setting the MW tidal field allows us to determine the Fornax tidal radius, $R_{\rm t}$, along its trajectory which, along its trajectory, represents an indication of its boundary. A good approximation of this length is given by

$$R_{\rm t} = \left(\frac{GM_{\rm F}}{\omega^2 + (\mathrm{d}^2\Phi_{\rm MW}/\mathrm{d}r^2)_{R_{\rm F_p}}} \right)^{1/3}, \tag{7}$$

where $M_{\rm F}$ is the Fornax mass, ω is its angular velocity (assumed constant) and $R_{\rm F_p}$ is the Fornax pericentre distance. Assuming $M_{\rm F} = 10^8$ M$_\odot$ and $R_{\rm F_p} = 138$ kpc (Buonanno et al. 1999), we obtained $R_{\rm t} = 5$ kpc.

2.2 The Fornax dSph model

According to observational data, a suitable expression for the Fornax mass density profile is a slightly modified Dehnen's law (Dehnen 1993):

$$\rho(r) = \frac{(3-\gamma)M_{\rm F}}{4\pi r_{\rm F}^3 \cosh(r/r_{\rm cut})} \left(\frac{r}{r_{\rm F}}\right)^{-\gamma} \left(\frac{r}{r_{\rm F}} + 1\right)^{-4+\gamma}, \tag{8}$$

where, again, $M_{\rm F}$ is the Fornax mass, $r_{\rm F}$ is its scale radius, and γ defines the inner slope of the density profile. The modification comes from the hyperbolic cosine at denominator, which allows an exterior cut in the sampling by particles, whose length-scale is given by $r_{\rm cut}$.

We developed two models with characteristics in agreement with observations, assuming (model D05) $M_{\rm F} = 1.48 \times 10^8$ M$_\odot$, $r_{\rm F} = 0.301$ kpc and $\gamma = 0.5$, and (model D1) $M_{\rm F} = 1.48 \times 10^8$ M$_\odot$, $r_{\rm F} = 0.391$ kpc and $\gamma = 1$.

These choices lead to models characterized by a radial mass profile in good agreement with observed mass estimates based on kinematical data, as shown in Fig. 1. It is worth noting that the two profiles are almost indistinguishable for $r > 1$ kpc. Table 2 summarizes the parameter choices we made for both models D05 and D1.

Table 2. Main parameters of the Fornax dSph model. Column 1: model name. Column 2: total mass of the model. Column 3: model scale radius. Column 4: slope of the density profile. Column 5: truncation radius. Column 6: mass enclosed within $r_{\rm cut}$. Column 7: number of particles used to model the system.

ID	$M_{\rm F}$ (10^8 M$_\odot$)	$r_{\rm F}$ (kpc)	γ	$r_{\rm cut}$ (kpc)	$M_{\rm cut}$ (10^8 M$_\odot$)	N
D05	1.48	0.301	0.5	2	1.06	967 889
D1	1.48	0.391	1.0	2	1.06	967 188

Table 3. Main observed properties of the Fornax GCs. Column 1: GC name. Column 2: mass of the GC. Column 3: projected distance to the Fornax centre. Column 4: line-of-sight velocity with respect to the Fornax centre of velocity. Column 5: GC core radius.

ID	$M_{\rm GC}$ (10^5 M$_\odot$)	$R_{\rm GC}$ (kpc)	$v_{\rm GC}$ (km s^{-1})	$r_{\rm GC,c}$ (pc)
GC1	0.37	1.60	–	5.01
GC2	1.82	1.05	-1.2 ± 4.6	5.81
GC3	3.63	0.43	7.1 ± 3.9	1.60
GC4	1.32	0.24	5.9 ± 3.4	1.75
GC5	1.78	1.43	8.7 ± 3.6	1.38

2.3 The GC models

To model the Fornax GCs, we used data collected in several papers (Hodge 1961; Rodgers & Roberts 1994; Mackey & Gilmore 2003; Cole et al. 2012), as summarized in Table 3.

The initial conditions for GC velocities are picked from the energy-dependent distribution function that gives the background density of equation (8). Under this requirement, we added the constraint that the GC positions in the x–y plane are the same as observed, and that the z component of the velocity is equal to the observed line-of-sight velocity. Moreover, we required that the GC 3D spatial positions are close to their observed projected positions.

While the other choices are dictated by observational constraints, the latter assumption is related to the so-called Fornax timing problem. The problem is that the Fornax GC ages are significantly greater than their estimated df decay times, which makes their present observed positions highly unlikely in the galaxy. As pointed out above, one of the solutions proposed to solve such a puzzle is the claim that GC df decay leads them to stall many Gyr ago in the case of a Fornax cored density profile (Read, Pontzen & Viel 2006a; Cole et al. 2012). Indeed, as shown by Gualandris & Merritt (2008), df stalls in cored systems when the satellite mass equals the galactic mass enclosed within its orbits. This also holds for cusped density profiles, although with some quantitative differences (Arca-Sedda & Capuzzo-Dolcetta 2014b).

Assuming, thus, that GC infall ceased many Gyr ago, in order for GCs to survive they needed to resist again tidal shattering for, at least, 20 orbital revolution around the Fornax nucleus. This could be because the GC ages are all around ∼10 Gyr and the Fornax crossing time is, roughly, $\sim\sqrt{R_{\rm t}^3/M_{\rm F}} = 0.4$ Gyr. A strong tidal field would have, on the other hand, likely shattered the clusters after just few orbital periods (Arca-Sedda et al. 2016). Therefore, the choice of setting $z = 0$, which maximizes both tidal forces and df effects, allows us a cleaner view of how these two processes affect the GC dynamics. In addition, it is worth noting that the likelihood that GC spatial and projected positions are close to each other has been already proposed by several authors to support the possibility

Table 4. Main parameters of GCs in model D05. Column 1: name of the GC. Column 2: adimensional potential well. Column 3: total mass. Column 4: radial distance to the Fornax centre. Column 5: tidal radius. Column 6: velocity dispersion. Column 7: central density. Column 8: number of particle used to model the GC. Column 9: orbital eccentricity. Column 10: df time-scale evaluated through equation (9). Column 11: tidal disruption time-scale as extrapolated from Fig. 4.

ID	$W0$	M_{GC} (10^5 $M_\odot$)	r_{GC} (kpc)	$r_{GC,t}$ (pc)	σ (km s^{-1})	Log ρ_0 ($M_\odot$ pc^{-3})	N	e	τ_{df} (Gyr)	τ_{td} (Gyr)
					Model D05					
GC1	4.9	0.37	1.60	102	1.25	0.41	3346	0.6	21.4	7
GC2	7.1	1.82	1.05	200	1.92	1.26	16 463	0.3	16.3	20
GC3	7.5	3.63	0.44	82	4.36	3.09	32 837	0.8	1.6	2.0
GC4	6.7	1.32	0.42	50	3.39	2.79	11 940	0.6	0.6	2.0
GC5	8.6	1.78	1.45	151	2.26	2.65	16 101	0.4	6.9	12.0
					Model D1					
GC1	4.6	0.37	1.61	91	1.32	1.46	3376	0.9	4.4	0.3
GC2	6.4	1.82	1.48	144	2.33	1.42	16 606	0.7	2.8	0.5
GC3	7.5	3.63	0.55	83	4.33	3.08	33 121	0.0	0.6	0.7
GC4	6.3	1.32	0.54	38	3.85	2.90	12 044	1.0	0.2	3.2
GC5	9.3	1.78	2.42	220	1.86	2.48	16 241	0.7	19.1	2.8

that they all formed within the Fornax tidal radius (Cole et al. 2012; Arca-Sedda & Capuzzo-Dolcetta 2016).

The internal structure of the GCs is represented by King models (King 1966), which are fully defined by the GC mass, M_{GC}, its adimensional potential well (W_0), and the concentration parameter (c), defined as the ratio between the GC core radius, $r_{GC,c}$, and its tidal radius, $r_{GC,t}$. To obtain the tidal radius of each cluster, we used equation (7) that is conveniently modified, whereas for $r_{GC,c}$ we assumed the estimates provided by observations (Mackey & Gilmore 2003). The knowledge of these two quantities allowed us to get W_0 since it is directly related to c.

Table 4 lists all the orbital and structural parameters for our models.

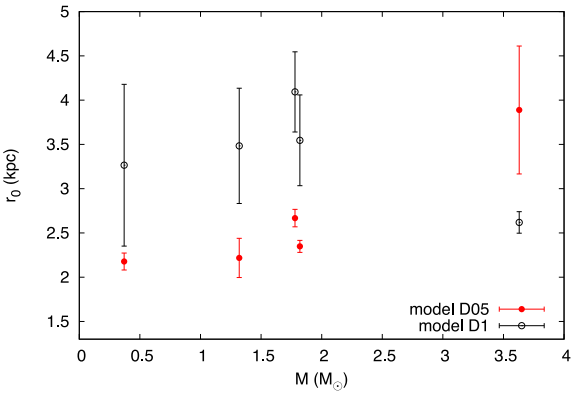

Figure 2. Initial radial positions of the GCs in model D05 (filled red circles) and model D1 (open black circles). The error bars are obtained assuming a 25 per cent error on the evaluation of the orbital eccentricity.

3 RESULTS

3.1 The role of dynamical friction

In the framework of the dry-merging scenario, the main process that drives the formation of an NC is df (Tremaine et al. 1975; Capuzzo-Dolcetta 1993). Using a series of highly resolved N-body simulations, Arca-Sedda & Capuzzo-Dolcetta (2014b) developed a fitting formula for the time, τ_{df}, needed to drag a body of mass M towards the centre of its parent galaxy. Such fitting formula has been improved recently by Arca-Sedda et al. (2015):

$$\tau_{df}\,(\mathrm{Myr}) = 0.3\sqrt{\frac{r_F^3\,(\mathrm{kpc}^3)}{M_F\,(10^{11}\,M_\odot)}}\,g(e,\gamma)\left(\frac{M}{M_F}\right)^{-0.67}\left(\frac{r}{r_F}\right)^{1.76}, \quad (9)$$

where e is the orbital eccentricity and

$$g(e,\gamma) = (2-\gamma)\left[a_1\left(\frac{1}{(2-\gamma)^{a_2}+a_3}\right)(1-e)+e\right], \quad (10)$$

with $a_1 = 2.63 \pm 0.17$, $a_2 = 2.26 \pm 0.08$ and $a_3 = 0.9 \pm 0.1$.

Equation (9) is particularly well suited in describing the orbital decay in galaxies characterized by cusped density profiles, though it has been shown that the formula also holds for cored systems.

Equation (9), applied to the GCs of model D05 and D1, gives a preliminary estimate of the time, τ_{df}, they need to plunge in the innermost region of the galaxy.

Table 4 lists τ_{df} for the GCs in models D05 and D1. In most of the cases, τ_{df} exceeds 1 Gyr.

Moreover, equation (9) can be used to make a guess about the radial positions, r_0, of the GCs at their birth. Indeed, for a given Dehen's galaxy model and for a given value of e, the difference between the GC initial decay time and its current value, estimated according to its present position r, is an approximate value of its age, τ. This means $\tau = \tau_{df}(r_0) - \tau_{df}(r)$, which, when solved for r_0, gives an estimate of the GC birthplace at a galactocentric distance:

$$r_0 = r\left(1+\frac{\tau}{\tau_{df}(r)}\right)^{0.57}. \quad (11)$$

Fig. 2 shows the initial positions of our GCs obtained in this way for each of the two models considered. The error bars are obtained assuming an error over the eccentricity of ∼25 per cent. These semi-analytical results are strong hints in favour of an *in situ* origin for all the clusters in both models because all the clusters have $r_0 < R_t$, where $R_t = 5$ kpc.

We carried out our simulations up to ∼3 Gyr for both the models discussed below.

In model D05, this time is twice the time needed for the decay of the heaviest GCs, which are the only contributing parameters to the formation of a nucleus.

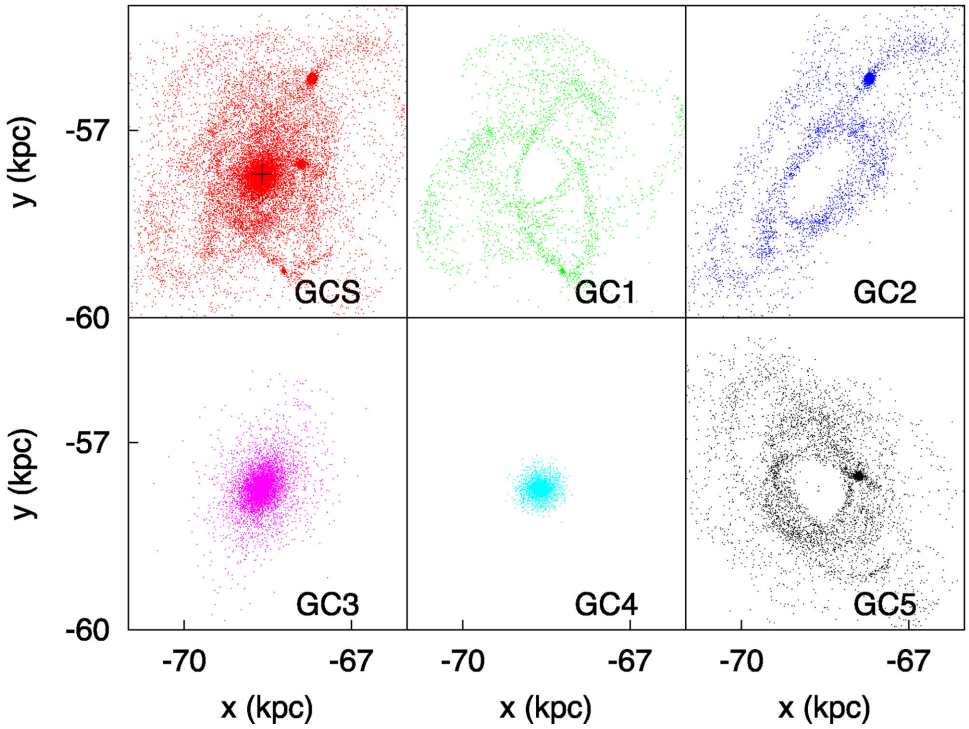

Figure 3. The Fornax GCS after 3.1 Gyr in model D05 in the MW reference frame. The whole GCS is represented in the top panel on the left column, whereas the five GCs are represented from top to bottom and from left to right in each one of the other panels. The white filled circle in the left corner top panel identifies the Fornax centre of density.

On the other hand, in model D1, the GC orbital infall and disruption are much faster, occurring in $\lesssim$1 Gyr. In this case, we carried out the simulation up to 3 Gyr in order to investigate whether the GC remnant can slowly deposit around the Fornax centre and give rise to a detectable nucleus.

3.2 Model D05

In this case, the Fornax density profile is significantly shallower than what expected from standard CDM predictions.

In order to highlight the effect of tidal forces and df of the GC motion, we show a snapshot at 3.1 Gyr of the various GCs in Fig. 3. Looking at the figure, it is evident that tidal forces have significantly acted on clusters GC1, GC2 and GC5. However, while GC2 and GC3 keep a clearly visible core, GC1 is almost completely dispersed along its orbit. On the other hand, clusters GC3 and GC4 have been able to reach the centre of Fornax, thus contributing to the formation of a compact structure. Note that in this case the coordinates of the Fornax centre in the MW reference frame are -68.5, -58, -161 kpc in the MW reference frame, as highlighted in the figure.

If we look at the GCS as a whole, which is shown in the top left panel of the figure, we find that merging of GCs has produced a quite evident central structure, which is orbited by three small clumps, relics of GC1, GC2 and GC5.

The upper panel in Fig. 4 shows the evolution of the radial mass of GCs as a function of time. To estimate the GC mass, we evaluate its tidal radius at each time-step using equation (7), conveniently adapted to the GC motion within Fornax. Then, we assume that the GC mass is that enclosed within such radius.

The clusters GC3 and GC4 merge into the galactic centre within 1.5 Gyr, dragging there $\sim 2.6 \times 10^5$ and $\sim 0.5 \times 10^5$ $M_\odot$, respectively.

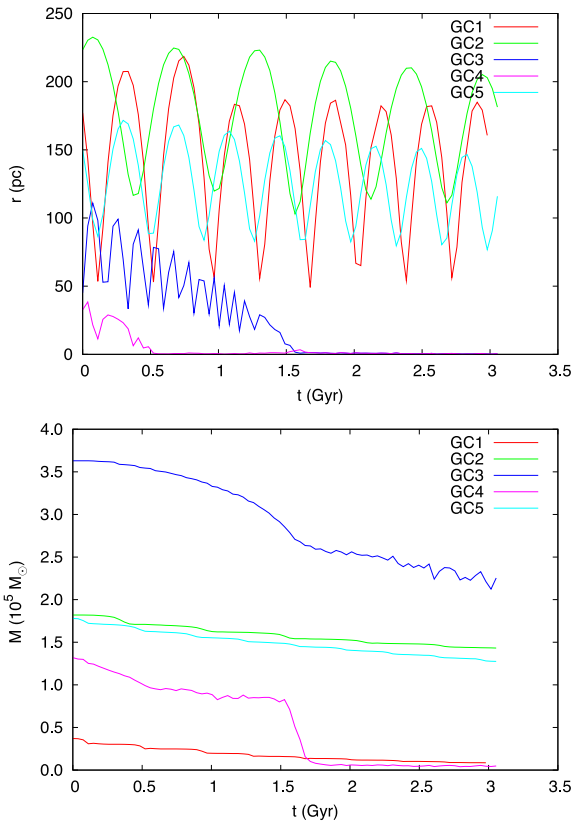

Figure 4. Time evolution of the radial distance to the Fornax centre (top panel) and of the total mass (bottom panel) for all the GCs in model D05.

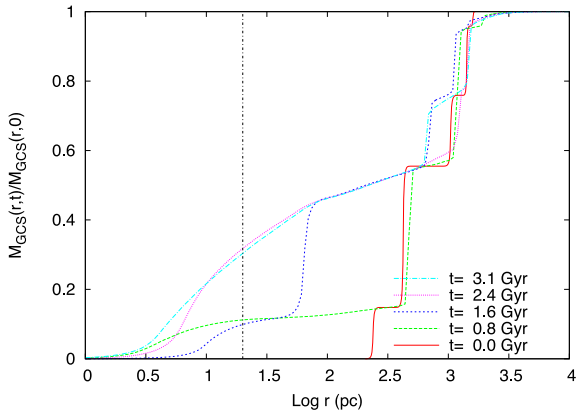

Figure 5. Cumulative mass distribution of the GCs at different times in model D05.

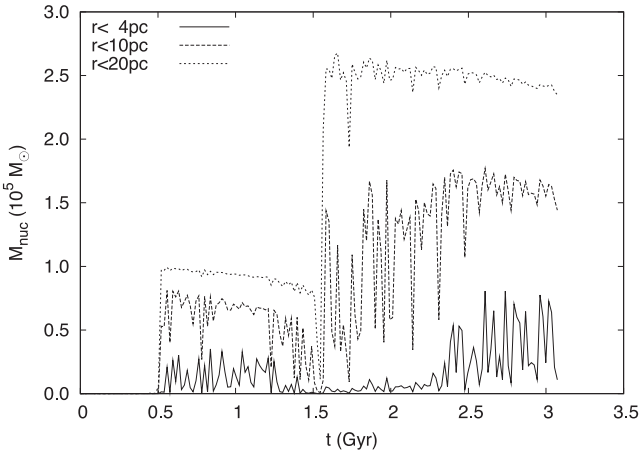

Figure 6. Mass deposited within 4 pc (straight line), 10 pc (dashed line) and 20 pc (dotted line) from the Fornax centre as a function of the time in model D05.

On the other hand, the bottom panel of Fig. 4 allows us to extrapolate the time at which the GC mass becomes smaller than 10^4 $M_\odot$, which we take as an estimate of the time required by the tidal action of the background stars to disrupt the incoming clusters (τ_{td}). In particular, we find $\tau_{td} < \tau_{df}$ for clusters GC1, GC2 and GC5 that means they poorly contribute to the formation of an NC.

Fig. 5 shows the mass distribution of the five GCs at different times; the mass enclosed within ∼20 pc saturates after 2 Gyr to a value that is ∼30 per cent of their total mass, i.e. $\simeq 2.6 \times 10^5$ $M_\odot$.

Some hints about the formation of an NC can be obtained looking at the amount of mass deposited into the galactic centre. For instance, Fig. 6 shows the mass enclosed within 4, 10 and 20 pc from the Fornax centre as a function of time. A steep increase that corresponds to the orbital decay of clusters GC2 and GC3 is evident.

To check whether the accumulated mass in model D05 leads to the formation of a detectable nucleus, we show its surface density profile in Fig. 7. The formation of a 'bright' nucleus characterized by an effective radius $r_{NC} \simeq (5.6 \pm 0.8)$ pc is evident. The enclosed mass is $M_{NC} \simeq (1.03 \pm 0.07) \times 10^5$ $M_\odot$.

3.3 Model D1

In the more centrally concentrated model D1, tidal forces acting on GCs are much more effective.

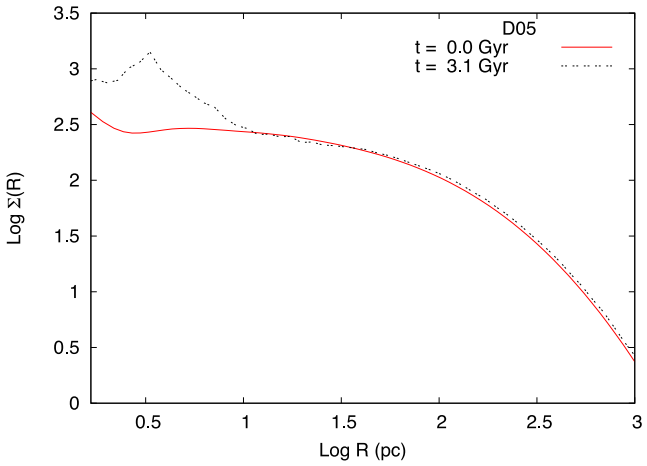

Figure 7. Surface density profile of the Fornax dSph at the beginning of the simulation and after 3.2 Gyr in model D05. A nucleus with effective radius $r_{NC} \simeq 5.6$ pc is evident.

Fig. 8 shows the whole GCS after 3.1 Gyr and also each cluster, making clear which of them contribute more to the formation of an NC. In this case, GC1 and GC5 are clearly disrupted by tidal forces, whereas GC2, GC3 and GC4 resist during their decay to the Fornax centre. In particular, it is worth noting that most of the mass lost by GC5 is deposited, after 3.1 Gyr, into the Fornax tidal tail, significantly contributing to its enhancement.

In Fig. 9, we compare the number distribution of the GC particles as a function of their distances from the Fornax centre, for both models D05 and D1. It is evident that in model D1 the GC5 cluster is completely disrupted, with some of its debris dispersed on distances beyond 15 kpc.

Surprisingly, we found that none of the clusters can deposit mass in the innermost region of Fornax ($r \lesssim 50$ pc). Indeed, the GC debris seem to distribute around a sort of 'hole'.

Actually, this region is not really empty since it contains background stars. Actually, it seems that the high density of the background prevents the deposit of mass in the innermost region of the galaxy. Hence, the background steep density profile acts as an MBH does in bright galaxies, suppressing the formation of a nucleus.

Indeed, a comparative look at the time evolution of the GC radial positions and masses (Fig. 10) shows that GC1 and GC2 are disrupted within 0.3 Gyr, well before they reach the inner 100 pc of the Fornax. Also, GC5 is almost completely disrupted from tidal forces in 0.5 Gyr. Clusters GC3 and GC4, instead, are able to reach the innermost region of the galaxy, though they suffer a loss of more than 80 per cent of their initial masses.

The efficiency of tidal forces is well evident in Fig. 11, which shows the cumulative mass distribution of the GCs at different times. Fig. 12 shows, indeed, that the orbital evolution of the GCs in this case does not lead to the formation of a detectable nucleus.

4 CONSEQUENCES FOR MBH FORMATION

In model D05, the GC orbital decay gives rise to a well-evident nucleus, whose surface density profile exceeds ∼5 times the background density. In particular, we show in Fig. 13 the cumulative radial mass distribution at $t = 0$ and after 3.1 Gyr for the whole system (Fornax + GCS). It is evident that the mass enclosed within 0.1 pc exceeds $M_{enc} = 10^3$ $M_\odot$, corresponding to a central density of $\sim 2 \times 10^5$ $M_\odot$ pc^{-3}. This value is about a hundred times higher

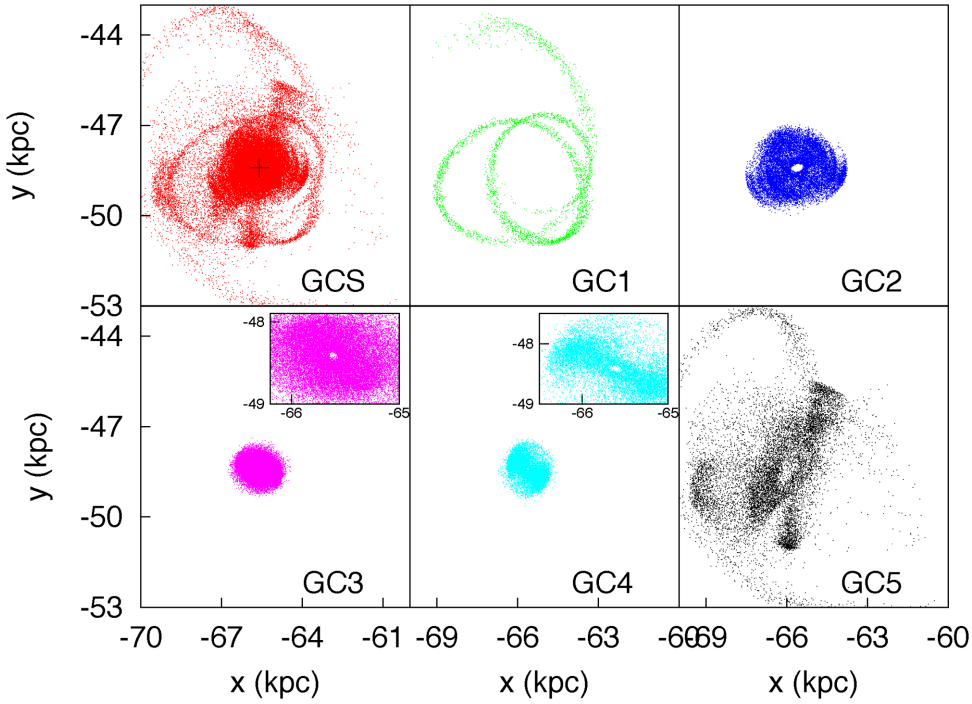

Figure 8. As in Fig. 3, but for model D1. In this case, looking at the zoomed panels contained in the bottom row, it is evident that GC3 and GC4 cannot penetrate the innermost region of Fornax. Indeed, in this case there is a hole in their centre.

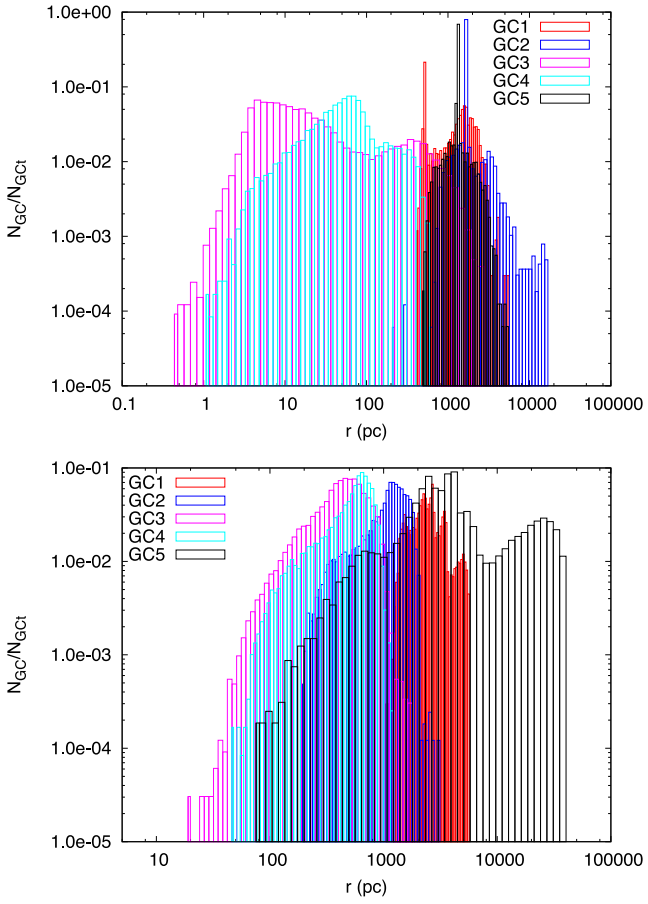

Figure 9. Fractional number of particles in each GC as a function of their distance to the Fornax centre. Top panel: model D05. Bottom panel: model D1.

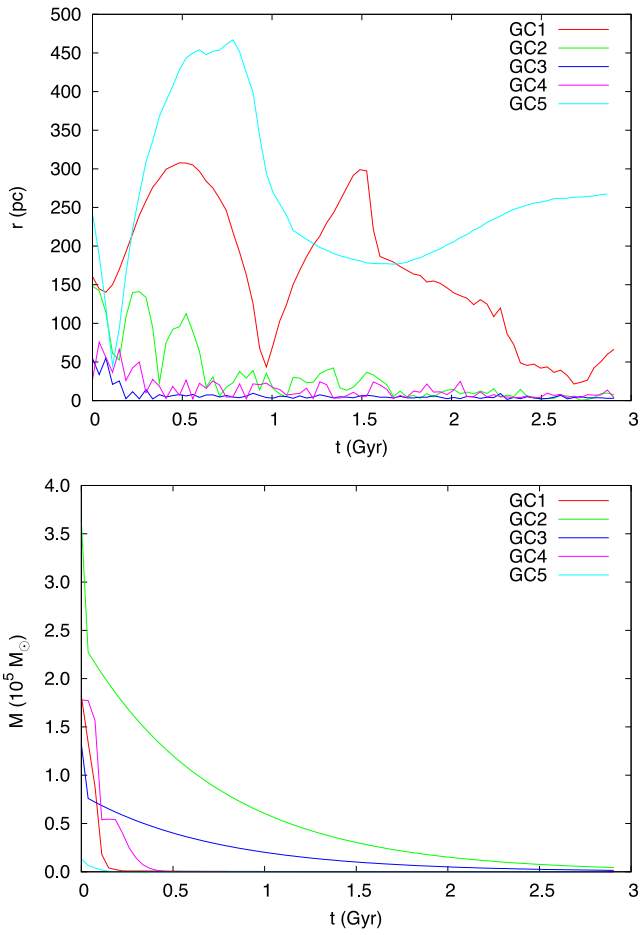

Figure 10. As in Fig. 4, but for model D1.

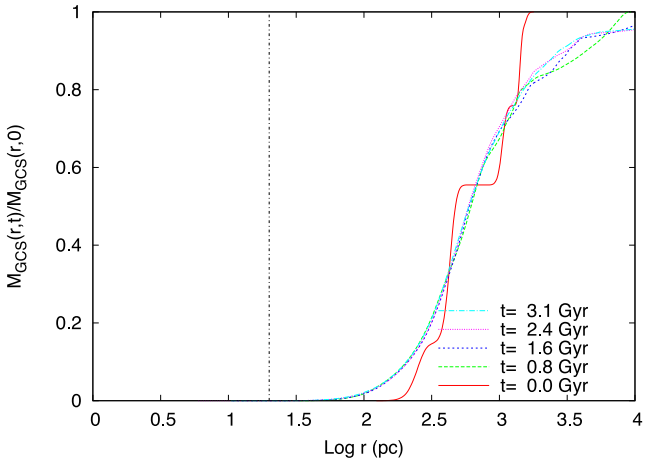

Figure 11. As in Fig. 5, but for model D1.

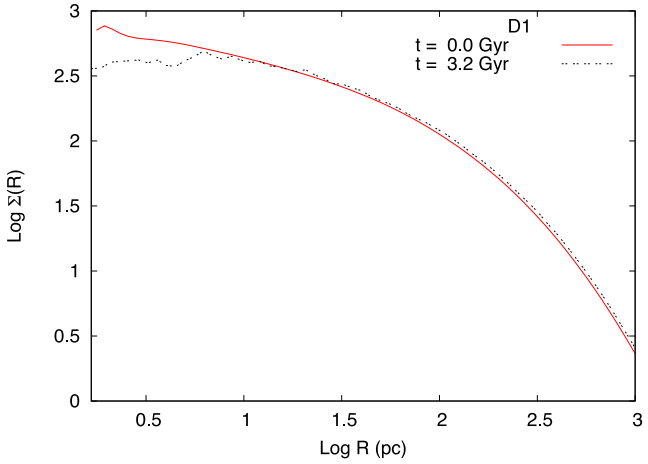

Figure 12. As in Fig. 7, but for model D1.

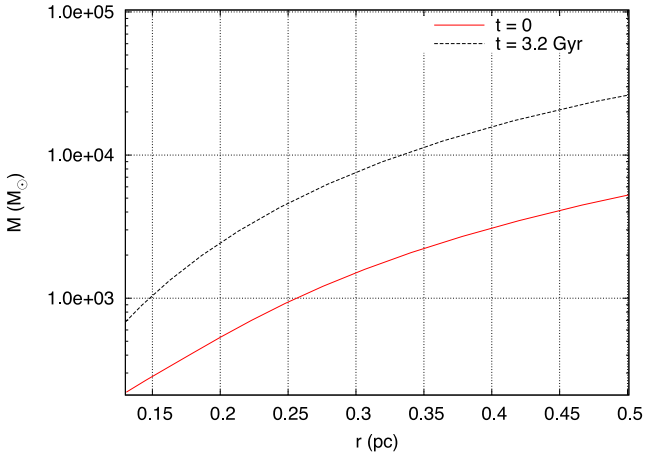

Figure 13. Enclosed mass as a function of radius for Fornax at the beginning of the simulation and after 3.1 Gyr for model D05.

than the initial central density of the most massive cluster, GC3, which is the one that contributes mostly to the NC formation.

As known, during their evolution GCs undergo mass segregation, which can lead to the formation of massive sub-systems in their cores, mainly composed of stellar BHs (see for example Spitzer 1969; Baumgardt et al. 2003, 2004; Arca-Sedda 2016 and reference therein). The subsequent evolution of such systems depends on the cluster properties and may lead, in some cases, to the formation of an MBH seed. This formation process has been usually invoked to explain the formation of the so-called intermediate-mass black holes (IMBHs), with masses ranging between 10^2 and 10^4 $M_\odot$, in dense and massive star clusters (Portegies Zwart & McMillan 2002; Freitag, Amaro-Seoane & Kalogera 2006; Gaburov, Gualandris & Portegies Zwart 2008; Mackey et al. 2008; Giersz et al. 2015; Arca-Sedda 2016).

In particular, for metal-poor systems, Arca-Sedda (2016) has shown that mass segregation drives the formation of a massive central system of evolved stars composed of ∼60 per cent of stellar BHs. Dynamical interactions among these BHs possibly leads to the formation of an IMBH seed under certain conditions (Giersz et al. 2015) but, in other cases, they can survive within the GC centre up to a Hubble time (Wang et al. 2016).

In any case, the formation of a dense sub-cluster of dark objects or an IMBH seed as a consequence of mass segregation and strong dynamical interactions is a process with typical time-scales that increase at increasing the mass of the host system. Indeed, this process occurs over several times the relaxation time-scale, which, approximately, scales with the host mass. For instance, for a typical galactic nucleus, the time-scale for such process easily exceeds a Hubble time. However, it is considerably smaller for smaller star clusters.

In this framework, our results can be used to investigate whether the orbital decay can lead to the formation, within the Fornax centre, of an MBH seed. As shown in Fig. 3, the formation of an NC is mainly due to the orbital decay of clusters GC3 and GC4. The scaling relation provided by Arca-Sedda (2016) suggests that these two metal-poor clusters should host at their centre two massive systems mainly composed of heavy stellar remnants, with masses of 2090 ± 48 and 758 ± 18 $M_\odot$, respectively, and sizes of ∼0.1 pc.

In its current version, our simulations cannot be used to follow stellar collisions, then we cannot state anything about the possible formation process of an IMBH. However, we can guess something about the possible accumulation of stellar BHs in the Fornax centre. Indeed, on the one hand, we know that mass segregation will lead to a significant deposit of heavy stellar BHs in the centre of the infalling GCs, while, on the other hand, we know from Fig. 9 that the particles that are deposited into the Fornax centre are those moving in the innermost region of the host cluster. Therefore, we expect that during the merging of GCs their cores, composed mainly of heavy stellar remnants, will collide together. The subsequent increase in the surrounding density can turn on a phase of strong dynamical interactions that can rapidly lead to the formation of a seed, as suggested by Giersz et al. (2015).

On the other hand, if at least one of the infalling GCs hosts an IMBH, which has formed during its past evolution, it should settle at the Fornax centre due to df, and subsequently may undergo a slow accretion phase.

It should be noted that if the IMBH is transported to the galactic centre by the infalling cluster, its mass will not scale with the host galaxy mass as expected for supermassive black holes (SMBHs) since in this case the central black hole would be significantly lighter. Indeed, for a Fornax-like system the expected mass for a central SMBH would be $M_{BH} = 1.5 \times 10^4$ $M_\odot$, according to the scaling relation provided by Scott & Graham (2013), 10 times heavier the mass of the infalling GC IMBH. Of course, such small IMBH would have poor effects on the surrounding nucleus, making its identification even more difficult.

Hence, if the dSph is characterized by a flat core or a shallow cusp at its formation, the decay and merging of its GCs can transport a significant amount of matter towards the galactic centre, causing an increase in the central density that can potentially favour the formation, or accretion, of an MBH. On the other hand, it should be noted that among all the dSph galaxies in the Local Group, only the Sagittarius dSph likely displays a nucleus in its centre despite its origin is still poorly understood. In this framework, hence, the absence of bright nuclei in dSphs would imply the absence of central MBHs but, at the same time, the possible future formation of such nuclei can facilitate the formation of a central IMBH.

5 IMPLICATIONS FOR THE CORE/CUSP PROBLEM

In this paper, we showed that the density profile of the Fornax dSph plays a fundamental role in determining the fate of its GCs. Indeed, we found that if Fornax is characterized by a steep density profile, its GCs will likely be disrupted in $\lesssim$1 Gyr. On the other hand, a shallower density profile would allow the formation of a relatively small NC, with a mass few times 10^5 $M_\odot$.

This allows some inference on the Fornax GCS history.

Indeed, let us make the, likely, hypothesis that the galaxy hosted, in the past, a larger population of clusters. Due to the fact that the additional GCs have already accomplished orbital decay, they should have had smaller apocentres than those of GCs presently observed. Anyway, our results suggest that, even if these GCs exist in the past, the efficient tidal action of the stellar background could have completely dispersed their debris, hiding the presence of any signature of their existence. This possibility represents an interesting alternative explanation for the so-called Fornax 'timing problem', which states that it is extremely unlikely that we are looking at the GCs just before their final sink to the Fornax centre. Indeed, it would imply that a steep stellar cusp in the galaxy centre can halt the formation of a nucleus, efficiently disrupting the infalling clusters and covering their past existence in the galactic background.

These results indicate that a galactic nucleus acts in the same way as SMBHs do, shattering the infalling GCs and halting the formation of a central nucleus (Capuzzo-Dolcetta 1993; Antonini 2013; Arca-Sedda et al. 2016). The effect of GC disruption operated by a steep cusp in the host galaxy density profile may be responsible for the observational absence of NCs in small dwarf galaxies (with masses around 10^8 $M_\odot$).

Interestingly, the absence of a nucleated region can tell us something about the luminous and dark matter content of the smallest, DM dominated, galaxies. Indeed, it is widely believed that dSph galaxies are characterized by large quantities of DM, but with density profiles significantly shallower than what expected by standard CDM paradigm. This is known as a core/cusp problem. One of the most credited scenarios proposes that initially a DMH form with a cuspy density profile, which is subsequently removed by merging events, tidal interaction with a larger galaxy, stellar formation, gas accretion and supernova (SN) explosions (see for example Mayer et al. 2001; Governato et al. 2012; Pontzen & Governato 2012; Yozin & Bekki 2012; Kazantzidis et al. 2013; Teyssier et al. 2013; Nipoti & Binney 2015; Pontzen et al. 2015 and reference therein). All these mechanisms can remove the initial DM cusp over timescales of the order of few Gyr, leaving the dSph with a nearly cored density profile, or, at least, a mild cusp ($\gamma \leq 0.6$).

In a recent work, Read, Agertz & Collins (2016) have shown that SN feedback and star formation drives the formation of a core on a time ~4 Gyr, a time which is fully compatible with the time-scale over which GC orbital decay can occur. This may imply that the cusp/core transformation is a complex process in which several different processes act together with an efficiency that likely depends on the host galaxy properties.

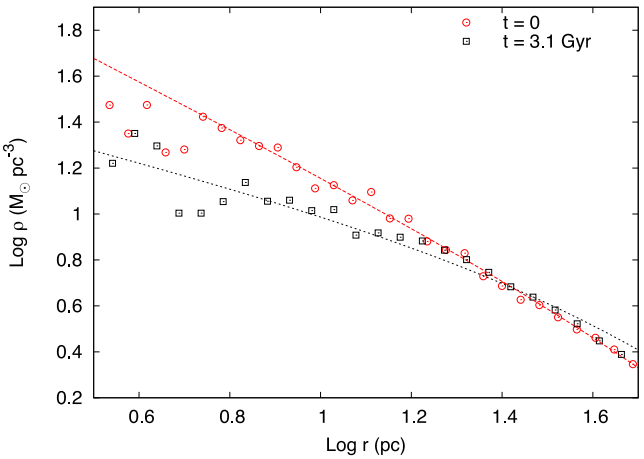

Figure 14. Density profile of the Fornax galaxy and its GCs at $t = 0$ and $t = 3.1$ Gyr in model D1. The initial cusp significantly flattens by the end of the simulation.

Moreover, another outcome of our results that can be related to the cusp/core problem is the following. Looking at model D05, we demonstrated that the future orbital decay of GCs will likely drive the formation of an NC, well visible as an edge in the surface density distribution. However, no clear signature of an NC is found in model D1. Indeed, looking closer to the Fornax centre, we found that its spatial density profile seems to flatten, as shown in Fig. 14. Surprisingly, a best fit of the density profile with a Dehnen model reveals two important modifications of the profile: (i) the scale radius decreases, passing from 391 to 285 $\pm$ 12 pc and (ii) the inner slope γ significantly decreases, passing from 1 to 0.65 $\pm$ 0.04. Therefore, the early orbital decay of GCs in DM-dominated dSph seems to be a complementary explanation for the core/cusp problem. This possible solution to the problem seems very general, as observations indicate that GC formation is a ubiquitous process occurring in all the galaxies. This alternative process for the cusp removal was first proposed by Goerdt et al. (2008, 2010). In particular, Goerdt et al. (2010) demonstrated that very massive, point-like satellites can remove the cusp in DMHs at very low densities ($\lesssim 10^{-2}$ $M_\odot$ pc^{-3}).

Despite the mechanism observed in our simulations is analogous to the one discovered by Goerdt et al. (2010), the crucial difference is that in this case it acts on relatively smaller scales, shaping the properties of dSph-sized systems. Moreover, our results suggest that the cusp/core transition can be operated by the orbital decay of 'normal' GCs, with masses $\lesssim 10^5$ $M_\odot$. More in detail, the models presented here are different for three main reasons:

(i) we modelled each GC using a reliable mass function as suggested by observations;

(ii) we modelled each GC by a sample of particles, thus accounting for their internal dynamics and their response to external tidal forces;

(iii) we modelled the evolution of relatively light GCs, with masses below 5×10^6 $M_\odot$, traversing a cuspy galaxy with typical density $\rho > 100$ $M_\odot$ pc^{-3}.

Even in such different conditions our results show that the sinking GCs can efficiently remove the cusp of a DM-dominated dSph.

6 DISCUSSION AND CONCLUSIONS

In this paper, we investigated the future evolution of the five GCs observed in the Fornax dSph. Our results suggest that the GC orbital decay can lead to a detectable NC only if the galaxy has a density profile shallower than r^{-1}. Otherwise, the galactic density cusp acts as a tidal heater, efficiently disrupting the incoming clusters before they can reach the galactic centre and deposit mass therein to give rise to a detectable nucleus.

Extending our results to a generic dSph that host some GCs close to its centre, we have shown that the GC infall can facilitate the accumulation of stellar BHs within the galactic central region, as well as of an IMBH formed during the past GC evolution. This would have implications on the possible BH–galaxy mass scaling relation, since for dSph the central black holes would be significantly lighter than expected and hardly detectable through usual 'dynamical estimators', such as the projected velocity dispersion (van der Marel & Anderson 2010; Haggard et al. 2013). Moreover, we have shown that if the dSph has a steep cusp at its birth, as expected by cosmological simulations, clusters traversing the galactic region are efficiently disrupted by tidal forces, thus quenching the formation of an NC. This would explain the absence of bright nuclei in the dSphs in the Local Group. Indeed, one possible path to the dSph formation and evolution is the following:

(i) the dSph forms with a steep cusp in the density profile and some GCs form following the overall galactic distribution;
(ii) due to df and tidal forces, loose GCs moving on inner orbits are efficiently disrupted, leaving almost untouched only those moving out of the galaxy scale radius;
(iii) the cusp distribution transforms into a cored one, as a consequence of some process, as explained in Section 5;
(iv) the surviving clusters undergo df and, due to the reduced efficiency of tidal forces, eventually reach the galactic centre and drive the formation of a bright nucleus.

In this picture, the GC tidal disruption could represent an efficient process for transforming the cuspy profile into a flatter one, as shown in the previous section.

In the following, we briefly summarize the main outcomes of this work:

(i) using highly resolved, direct, *N*-body simulations, based on observations of the Fornax dSph, we modelled the evolution of a GCS within the Fornax dSph galaxy, representing in a reliable way both the clusters and the parent galaxy;
(ii) we have shown that if the dSph has a shallow cusp in the density profile, the GC orbital decay leads to the formation of a detectable nucleus over a time-scale of 1.5 Gyr, with properties similar to those expected by extrapolation of observational scaling relations valid for heavier galaxies;
(iii) on the other hand, if the dSph has a cuspy density profile, as suggested by CDM predictions, tidal forces are strong enough to disrupt the infalling clusters, thus preventing the formation of an NC;
(iv) in the case of nearly cored dSphs, we expect that GC decay and merging can favour the formation of an IMBH, especially if one of the GCs contains an IMBH previously formed, this would imply a BH–galaxy mass relation substantially steeper at low galaxy mass, with BH masses significantly smaller than expected from observational scaling relations based on heavier galaxies data;
(v) in the case of cuspy dSphs, instead, we showed that the GC tidal disruption significantly affects the background mass distribution. In particular, the density profile significantly flattens. This process can play an interesting role in the solution of the core/cusp problem;
(vi) the missing observational evidence of nuclei in the LG dSphs would imply that dSphs have formed with a steep cusp, thus disrupting all those clusters formed within the galactic scale radius; after the transformation of the cusp into a core, only the surviving clusters can lead to the formation of a nucleus, but on a significantly longer time-scale, since they formed in an outer region of the galaxy;
(vii) finally, we suggest that dSph may follow a well-determined evolutionary path: (1) they form with a steep density profile, (2) the innermost star clusters are disrupted by tidal forces and, in turn, they flatten the galactic density profile, (3) at this point, farther GCs can reach the galactic centre and (4) contribute to the formation of a nucleus.
(viii) The clear dearth of bright nuclei in the LG dSph population may indicate that the first part of the evolutionary process [points (i) and (ii)] has a very long time, as also suggested by simulations.

ACKNOWLEDGEMENTS

MAS acknowledges financial support from the University of Rome 'Sapienza' through the grant'52/2015' in the framework of the research project 'MEGaN: modelling the environment of galactic nuclei'. Part of this work was performed at the Aspen Center for Physics, which is supported by National Science Foundation grantPHY-1066293. In this regard, RCD thanks the Simons Foundation for the grant that allowed him a period at the Aspen Center for Physics where he developed part of this work.

REFERENCES

Aharon D., Perets H. B., 2015, ApJ, 799, 185
Allen C., Santillan A., 1991, Rev. Mex. Astron. Astrofis., 22, 255
Angus G. W., Diaferio A., 2009, MNRAS, 396, 887
Antonini F., 2013, ApJ, 763, 62
Antonini F., Merritt D., 2012, ApJ, 745, 83
Antonini F., Capuzzo-Dolcetta R., Mastrobuono-Battisti A., Merritt D., 2012, ApJ, 750, 111
Arca-Sedda M., 2016, MNRAS, 455, 35
Arca-Sedda M., Capuzzo-Dolcetta R., 2014a, MNRAS, 444, 3738
Arca-Sedda M., Capuzzo-Dolcetta R., 2014b, ApJ, 785, 51
Arca-Sedda M., Capuzzo-Dolcetta R., 2016, MNRAS, 461, 4335
Arca-Sedda M., Capuzzo-Dolcetta R., Antonini F., Seth A., 2015, ApJ, 806, 220
Arca-Sedda M., Capuzzo-Dolcetta R., Spera M., 2016, MNRAS, 456, 2457
Baumgardt H., Hut P., Makino J., McMillan S., Portegies Zwart S., 2003, ApJ, 582, L21
Baumgardt H., Makino J., Ebisuzaki T., 2004, ApJ, 613, 1143
Bekki K., Graham A. W., 2010, ApJ, 714, L313
Buonanno R., Corsi C. E., Zinn R., Pecci F. F., Hardy E., Suntzeff N. B., 1998, ApJ, 501, L33
Buonanno R., Corsi C. E., Castellani M., Marconi G., Fusi Pecci F., Zinn R., 1999, AJ, 118, 1671
Capuzzo-Dolcetta R., 1993, ApJ, 415, 616
Capuzzo-Dolcetta R., Miocchi P., 2008, ApJ, 681, 1136
Capuzzo-Dolcetta R., Spera M., Punzo D., 2013, J. Comput. Phys., 236, 580
Chandrasekhar S., 1943, ApJ, 97, 255
Cole D. R., Dehnen W., Read J. I., Wilkinson M. I., 2012, MNRAS, 426, 601
Coleman M., Da Costa G. S., Bland-Hawthorn J., Martínez-Delgado D., Freeman K. C., Malin D., 2004, AJ, 127, 832
Côté P. et al., 2004, ApJS, 153, 223
Côté P. et al., 2006, ApJS, 165, 57
Cowsik R., Wagoner K., Berti E., Sircar A., 2009, ApJ, 699, 1389

Dehnen W., 1993, MNRAS, 265, 250
Dinescu D. I., Keeney B. A., Majewski S. R., Girard T. M., 2004, AJ, 128, 687
Flores R. A., Primack J. R., 1994, ApJ, 427, L1
Freitag M., Amaro-Seoane P., Kalogera V., 2006, J. Phys. Conf. Ser., 54, 252
Gaburov E., Gualandris A., Portegies Zwart S., 2008, MNRAS, 384, 376
Giersz M., Leigh N., Hypki A., Lützgendorf N., Askar A., 2015, MNRAS, 454, 3150
Gilmore G., Wilkinson M. I., Wyse R. F. G., Kleyna J. T., Koch A., Evans N. W., Grebel E. K., 2007, ApJ, 663, 948
Goerdt T., Moore B., Read J. I., Stadel J., Zemp M., 2006, MNRAS, 368, 1073
Goerdt T., Moore B., Kazantzidis S., Kaufmann T., Macciò A. V., Stadel J., 2008, MNRAS, 385, 2136
Goerdt T., Moore B., Read J. I., Stadel J., 2010, ApJ, 725, 1707
Governato F. et al., 2012, MNRAS, 422, 1231
Gualandris A., Merritt D., 2008, ApJ, 678, 780
Haggard D., Cool A. M., Heinke C. O., van der Marel R., Cohn H. N., Lugger P. M., Anderson J., 2013, ApJ, 773, L31
Hodge P. W., 1961, AJ, 66, 83
Jardel J. R., Gebhardt K., 2012, ApJ, 746, 89
Kazantzidis S., Łokas E. L., Mayer L., 2013, ApJ, 764, L29
King I. R., 1966, AJ, 71, 64
Larsen S. S., Strader J., Brodie J. P., 2012, AAP, 544, L14
Leigh N., Böker T., Knigge C., 2012, MNRAS, 424, 2130
Mackey A. D., Gilmore G. F., 2003, MNRAS, 340, 175
Mackey A. D., Wilkinson M. I., Davies M. B., Gilmore G. F., 2008, MNRAS, 386, 65
Mateo M. L., 1998, ARA&A, 36, 435
Mayer L., Governato F., Colpi M., Moore B., Quinn T., Wadsley J., Stadel J., Lake G., 2001, ApJ, 559, 754
McLaughlin D. E., King A. R., Nayakshin S., 2006, ApJ, 650, L37
Milgrom M., 1983, ApJ, 270, 365
Miyamoto M., Nagai R., 1975, PASJ, 27, 533
Moore B., 1994, Nature, 370, 629
Navarro J. F., Frenk C. S., White S. D. M., 1996, ApJ, 462, 563
Nayakshin S., Wilkinson M. I., King A., 2009, MNRAS, 398, L54
Nipoti C., Binney J., 2015, MNRAS, 446, 1820
Oh K. S., Lin D. N. C., Richer H. B., 2000, ApJ, 531, 727
Olszewski E. W., Mateo M., Harris J., Walker M. G., Coleman M. G., Da Costa G. S., 2006, AJ, 131, 912
Ostriker J. P., Binney J., Saha P., 1989, MNRAS, 241, 849
Pesce E., Capuzzo-Dolcetta R., Vietri M., 1992, MNRAS, 254, 466
Petts J. A., Gualandris A., Read J. I., 2015, MNRAS, 454, 3778
Petts J. A., Read J. I., Gualandris A., 2016, MNRAS
Plummer H. C., 1911, MNRAS, 71, 460
Pontzen A., Governato F., 2012, MNRAS, 421, 3464
Pontzen A., Read J. I., Teyssier R., Governato F., Gualandris A., Roth N., Devriendt J., 2015, MNRAS, 451, 1366
Portegies Zwart S. F., McMillan S. L. W., 2002, ApJ, 576, 899
Read J. I., Pontzen A. P., Viel M., 2006a, MNRAS, 371, 885
Read J. I., Goerdt T., Moore B., Pontzen A. P., Stadel J., Lake G., 2006b, MNRAS, 373, 1451
Read J. I., Agertz O., Collins M. L. M., 2016, MNRAS, 459, 2573
Rodgers A. W., Roberts W. H., 1994, AJ, 107, 1737
Scott N., Graham A. W., 2013, ApJ, 763, 76
Spitzer L., Jr, 1969, ApJ, 158, L139
Strigari L. E., Bullock J. S., Kaplinghat M., Kravtsov A. V., Gnedin O. Y., Abazajian K., Klypin A. A., 2006, ApJ, 652, 306
Teyssier R., Pontzen A., Dubois Y., Read J. I., 2013, MNRAS, 429, 3068
Tremaine S. D., 1976, ApJ, 203, 72
Tremaine S. D., Ostriker J. P., Spitzer L., Jr1975, ApJ, 196, 407
Turner M. L., Côté P., Ferrarese L., Jordán A., Blakeslee J. P., Mei S., Peng E. W., West M. J., 2012, ApJS, 203, 5
van den Bergh S., 1986, AJ, 91, 271
van der Marel R. P., Anderson J., 2010, ApJ, 710, 1063
Walker M. G., Peñarrubia J., 2011, ApJ, 742, 20
Walker M. G., Mateo M., Olszewski E. W., Peñarrubia J., Wyn Evans N., Gilmore G., 2009, ApJ, 704, 1274
Wang L. et al., 2016, MNRAS, 458, 1450
Wolf J., Martinez G. D., Bullock J. S., Kaplinghat M., Geha M., Muñoz R. R., Simon J. D., Avedo F. F., 2010, MNRAS, 406, 1220
Yozin C., Bekki K., 2012, ApJ, 756, L18

This paper has been typeset from a TEX/LATEX file prepared by the author.